Available online at www.sciencedirect.com
SCIENCE DIRECT
Journal of Catalysis 228 (2004) 234–242
JOURNAL OF CATALYSIS
www.elsevier.com/locate/jcat

Solid-state MAS NMR studies on the hydrothermal stability of the zeolite catalysts for residual oil selective catalytic cracking

Jianqin Zhuang [1], Ding Ma [2], Gang Yang, Zhimin Yan, Xiumei Liu, Xianchun Liu, Xiuwen Han, Xinhe Bao *, Peng Xie, and Zhongmin Liu

State Key Laboratory of Catalysis, Dalian Institute of Chemical Physics, Chinese Academy of Sciences, Dalian 116023, China

Received 24 May 2004; revised 18 August 2004; accepted 23 August 2004

Abstract

By using the solid-state MAS NMR technique, the hydrothermal stabilities (under 100% steam at 1073 K) of HZSM-5 zeolites modified by lanthanum and phosphorus have been studied. They are excellent zeolite catalysts for residual oil selective catalytic cracking (RSCC) processes. It was indicated that the introduction of phosphorus to the zeolite via impregnation with orthophosphoric acid led to dealumination as well as formation of different Al species, which were well distinguished by ^{27}Al 3Q MAS NMR. Meanwhile, the hydrothermal stabilities of the zeolites (P/HZSM-5, La-P/HZSM-5) were enhanced even after the samples were treated under severe conditions for a prolonged time. It was found that the Si–O–Al bonds were broken under hydrothermal conditions, while at the same time the phosphorous compounds would occupy the silicon sites to form $(SiO)_x Al(OP)_{4-x}$ species. With increasing time, more silicon sites around the tetrahedral coordinated Al in the lattice can be replaced till the aluminum is completely expelled from the framework. The existence of lanthanum can partially restrict the breaking of the Si–O–Al bonds and the replacement of the silicon sites by phosphorus, thus preventing dealumination under hydrothermal conditions. This was also proved by ^{31}P MAS NMR spectra.

Keywords: Solid-state MAS NMR; Hydrothermal stability; Zeolites

1. Introduction

The upgrading of residual oil into light alkenes has attracted increasing interest since the market demand for ethylene, propylene, etc. is steadily growing, on the one hand, and more and more heavy fractions were explored in crude oil on the other hand [1]. This situation promoted the development of a novel technology, namely, residual oil selective catalytic cracking (RSCC) [2]. Compared with the traditional fluid catalytic cracking (FCC), the RSCC process is carried out under a higher temperature (953 K), and higher selectivity for light alkenes can be obtained. Normally, catalysts are regenerated in a steam environment at temperatures higher than the reaction temperature, and this makes steam stability an important factor in the catalysts used in the petroleum industry [3–6]. Therefore, the preservation of good activity and selectivity in the highly severe reaction and regeneration processes of RSCC requires the catalysts to maintain good thermal and hydrothermal stabilities. The HZSM-5 zeolite shows unique shape-selective properties and moderate acidity, and is usually used as catalyst additives in gas oil cracking, and plays a key role in enhancing the gasoline octane rating [7]. It has rather small (intermediate size) pore openings (5.5 Å), which restricts the access of branched and cyclic hydrocarbons from the matrix of the catalysts into its pores where the active sites are located, but allows straight chain and monomethyl paraffins to enter and be preferentially cracked to lighter products [6]. However, HZSM-5

* Corresponding author.
E-mail address: xhbao@dicp.ac.cn (X. Bao).
[1] Present address: BASF Aktiengesellschaft, D-67056 Ludwigshafen, Germany.
[2] Present address: School of Chemistry, University of Bristol, Bristol, BS8 1TS, UK.

0021-9517/$ – see front matter
doi:10.1016/j.jcat.2004.08.034

zeolite is not very stable under severe hydrothermal conditions for a long period of time. Incorporation of multivalent cations, such as rare-earth elements, or modification of the HZSM-5 zeolites by impregnation with H_3PO_4 [3,8–10], is normally used to enhance the hydrothermal stability of the framework, as well as to preserve the activity and selectivity for cracking [11,12]. It has been found that HZSM-5 zeolites modified with both lanthanum and phosphorus exhibit higher hydrothermal stabilities and excellent selectivities for light alkenes in the RSCC process [2]. However, owing to the complexity of the catalysts system, little is known about the interaction of the additives with the zeolite under hydrothermal conditions, which limited further improvement of the catalysts.

Solid-state MAS NMR is a powerful tool in the structural analysis of zeolites, especially for getting information of local structure, geometry, and coordination of the building atoms such as Si and O or the hetero-substitute atoms [13,14]. Particularly, with the application of the 2D ^{27}Al MQ (multiple-quantum) MAS NMR, the distribution of different Al sites in the configuration within the zeolite lattice can be well resolved from the broadened spectra caused by the second-order quadrupole interaction of the central transition [15–19]. It permits an unambiguous assignment of the aluminum coordinations in the spectra. The aim of the present paper is to investigate the interaction between the additives (La and P) and HZSM-5 zeolite, as well as the hydrothermal stabilities of these catalysts by means of the solid-state MAS NMR techniques.

2. Experimental

2.1. Preparation of samples

The HZSM-5 zeolites studied in the present work are commercial products. The sample with exchanged La was obtained from HZSM-5 by ion exchange with a $La(NO_3)_3$ solution. The ion-exchange procedure was as follows: a calculated amount of $La(NO_3)_3$ was dissolved in deionized water, and the HZSM-5 was then mixed with this solution and kept at 343 K with stirring for 10 h. The sample was then filtered, washed with deionized water, and dried in air at 383 K. The sample modified with phosphorus was carried out by impregnation with an aqueous solution of phosphoric acid (pH = 1). The impregnated sample was washed with deionized water, subsequently dried at 393 K, and then calcined at 813 K for 3 h. The La-P/HZSM-5 zeolitic catalyst was prepared by adding the P/HZSM-5 catalyst to a solution of $La(NO_3)_3$. Hydrothermal treatment of the samples was carried out in a quartz reactor tube. The temperature was increased at a rate of 10 K/min to the treatment temperature under dry nitrogen. Steam treatments were carried out at 1073 K for various durations of time, under a water vapor pressure of 0.1 MPa.

2.2. Physicochemical characterizations

The structure of the commercial zeolite was checked by a D/max-γb-type X-ray diffractometer (Rigaku) using monochromatic Cu$K\alpha$ radiation (40 kV and 100 mA), with a scan speed of 5°/min in 2θ. The crystallinity was determined by using HZSM-5 zeolite as the reference material and the total intensity of the strongest reflections in the region $15 < 2\theta < 36°$ [20]. Chemical analysis was performed using a Philips Magix 9148 X-ray fluorescence spectrometer.

2.3. NMR measurements

All NMR spectra were obtained at room temperature on a Bruker DRX-400 spectrometer with a BBO MAS probe head, using 4 mm ZrO_2 rotors. ^{29}Si MAS NMR spectra with high-power proton decoupling were recorded at 79.5 MHz using 1.6 μs pulse, 4 s repetition time, and 2048 scans. All ^{29}Si spectra were recorded on samples spun at 4 kHz and referenced to DSS. ^{27}Al MAS NMR spectra were recorded with high-power proton decoupling at 104.3 MHz using a 0.75 μs pulse, 2 s repetition time, and 1024 scans. ^{1}H MAS NMR spectra were obtained at 400.1 MHz by means of single-pulse experiments, with a 3 μs pulse, 4 s repetition time, and 100 scans. All ^{27}Al and ^{1}H MAS NMR spectra were recorded with samples spun at 8 kHz, and chemical shifts were referenced to 1% aqueous $Al(NO_3)_3$ and a saturated aqueous solution of DSS, respectively.

The ^{27}Al MQ MAS NMR spectra were used to determine the coordinations of the aluminum species present in the modified zeolite HZSM-5 samples [18,19]. The sample spinning rate was controlled at 9–10 kHz. To produce pure-absorption lineshapes, a three-pulse sequence was used and the phase cycling was designed to select the coherence pathway of $(0) \to (3) \to (0) \to (-1)$. The first and second pulses were individually optimized to give maximum efficiencies for the $0Q \to \pm 3Q$ coherence creation and the $\pm 3Q \to 0Q$ conversion steps, respectively. The first and the second pulse lengths were optimized to be 4 and 1.8 μs, respectively. The last conversion step ($0Q \to -1Q$) to the observed central transition was achieved by using a selective pulse of 20 μs duration. The spectra were recorded with 1024×256 data points and the frequency matrixes were 1024×256 before the 2D Fourier transform. For each t1 increment, 48 scans were used to accumulate the signals with a recycle delay of 2 s. A shearing transformation was performed after the 2D transform [21]. The chemical shift was referenced to an $Al(NO_3)_3$ aqueous solution at 0 ppm. The isotropic shift and the second-order quadrupolar effect (SOQE) were estimated from the spectrum with the following:

$$\delta_{\mathrm{iso}}(i) = \tfrac{4}{3}\delta_1(i) - \tfrac{1}{3}\delta_2(i), \tag{1}$$

$$\begin{aligned}\mathrm{SOQE}(i)^2 &= C_{\mathrm{q}}(i)^2\bigl(1+\eta(i)^2\bigr)/3 \\ &= \bigl[\delta_{\mathrm{iso}}(i) - \delta_2(i)\bigr]\nu_0^2/6000,\end{aligned} \tag{2}$$

Table 1
The XRF results of the HZSM-5 and modification zeolites

Zeolite	SiO_2 (%)	Al_2O_3 (%)	P_2O_5 (%)	La_2O_3 (%)	Fe_2O_3 (%)	Si/Al
HZSM-5	95.360	4.556	–	–	0.084	17.5
La/HZSM-5	94.662	4.513	–	0.734	0.091	17.5
P/HZSM-5	92.174	4.277	3.467	–	0.081	18.0
La-P/HZSM-5	90.608	4.294	4.041	0.972	0.084	17.6

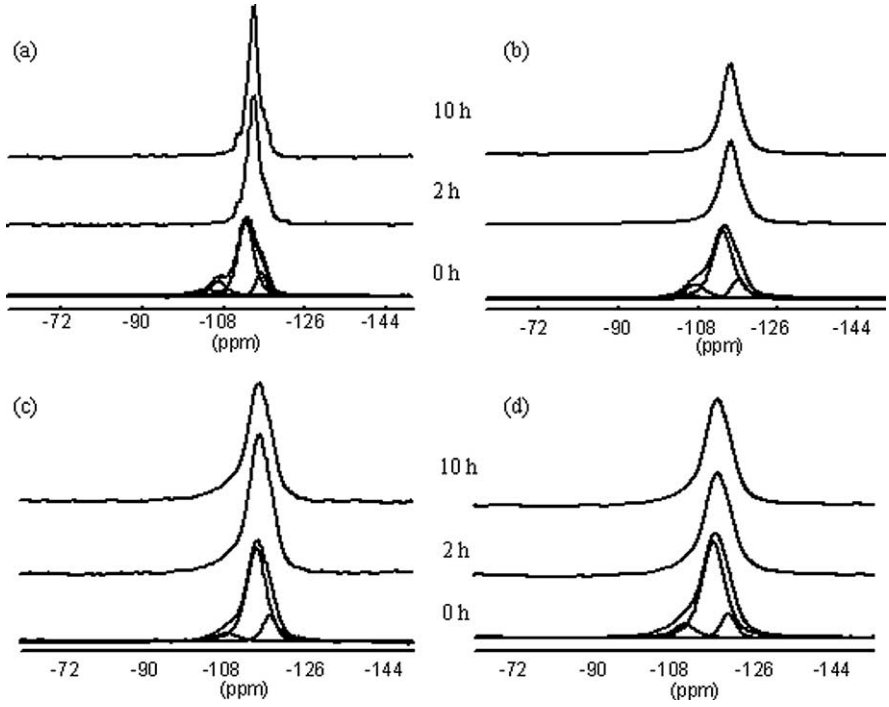

Fig. 1. ^{29}Si MAS NMR spectra of zeolites treated with 100% steam at 1073 K for different times: (a) HZSM-5, (b) La/HZSM-5, (c) P/HZSM-5, (d) La-P/HZSM-5.

where $\delta_{iso}(i)$ is the isotropic chemical shift and $\delta_1(i)$ and $\delta_2(i)$ are the coordinates for the center of gravity of signal i in the F_1 and F_2 dimensions, respectively; $C_q(i)$ is the quadrupolar coupling constant; $\eta(i)$ is the asymmetry parameter; and ν_0 is the Larmor frequency of ^{27}Al.

3. Results and discussion

3.1. Physicochemical characteristics of the samples

Table 1 lists the XRF results of the samples. Total Si/Al ratios, including both the framework and the extraframework species, were around 18. The structural and crystalline characteristics of the samples were studied by XRD. All the samples were well crystallized as the MFI structure, as deduced from the XRD spectra. Table 2 shows the relative crystallinity of the samples as compared to the parent HZSM-5 zeolite. No observable reduction in crystallinity of the HZSM-5 can be seen after the addition of lanthanum. On the other hand, the relative crystallinity decreased to a certain extent for those samples impregnated with orthophosphoric acid, and this might be due to the dealumination of the zeolites. When located under conditions of 100% steam at 1073 K for different times, the crystallinity of all the samples decreased, but those samples modified with additives showed a slower decrease under severe conditions, as compared to the parent HZSM-5 zeolite. The La-P/HZSM-5 sample could retain its stability for a long time despite the decrease in crystallinity during the first 2 h.

3.2. ^{29}Si MAS and ^{1}H MAS NMR spectra of the samples

The ^{29}Si MAS NMR spectra are shown in Fig. 1 for HZSM-5 zeolite as well as the samples modified with additives before and after hydrothermal treatment at 1073 K. It exhibits an intense and broad signal at −114.8 ppm, which is assigned to Q^4 [$Si(OSi)_4$] species, while the shoulder at −117.4 ppm is attributed to the presence of crystallographically inequivalent sites in the zeolite [22]. The peak centered at −107.4 ppm is assigned to the silicon atoms in the SiO_4 tetrahedral surrounded by three silicon atoms (3Si, 1Al). An unobvious resonance at −103.0 ppm could be recognized, which is related to the Q^3 [$Si(OSi)_3(OH)$] silicon atoms of

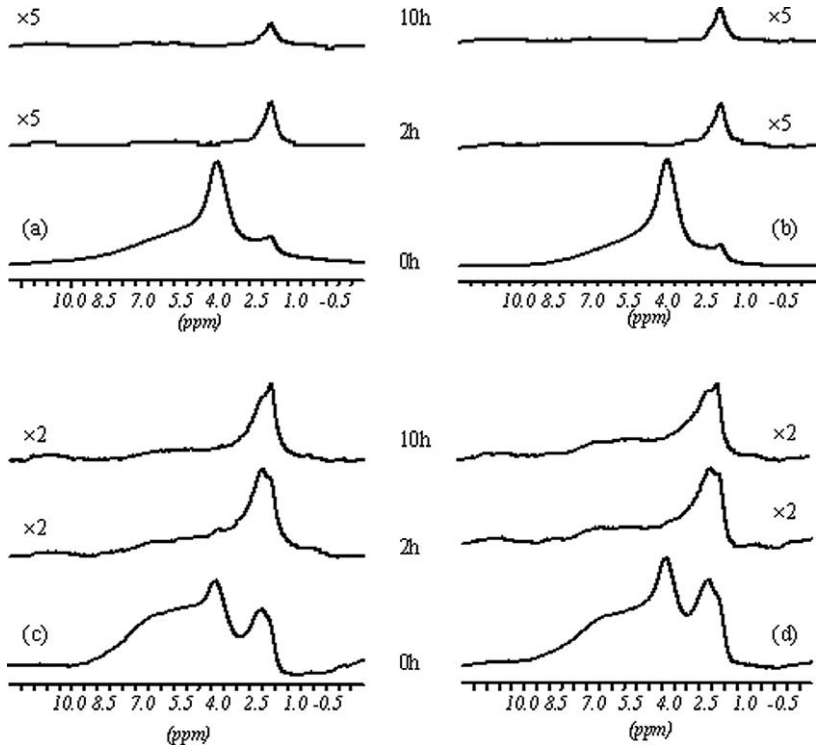

Fig. 2. ^{1}H MAS NMR spectra of zeolites treated with 100% steam at 1073 K for different times: (a) HZSM-5, (b) La/HZSM-5, (c) P/HZSM-5, (d) La-P/HZSM-5.

Table 2
Physicochemical characteristics of HZSM-5 and modification samples

Sample	Crystallinity[a] (%)	Si/Al[b] (NMR)
HZSM-5	100	21
HZSM-5 (2 h)[c]	88	–
HZSM-5 (10 h)	84	–
La/HZSM-5 (0 h)	100	21
La/HZSM-5 (2 h)	98	135
La/HZSM-5 (10 h)	92	–
P/HZSM-5 (0 h)	87	33
P/HZSM-5 (2 h)	85	53
P/HZSM-5 (10 h)	80	60
La-P/HZSM-5 (0 h)	84	33
La-P/HZSM-5 (2 h)	73	48
La-P/HZSM-5 (10 h)	72	57

[a] Based on XRD spectra.
[b] Calculated by ^{29}Si MAS NMR spectra.
[c] Represents the time of hydrothermal treatment at 1073 K.

silanol groups [22]. Van Bokhoven has reported that with the addition of La into the NaY zeolite, the silicon atoms in the direct vicinity of the lanthanum ions would feel its presence and undergo a large shift due to the very strong electrostatic interaction of the lanthanum with the zeolite framework. The overall spectrum also showed a small gradual change in peak position to a higher field with higher weight percentage of lanthanum [23]. However, there was no shift observed in our ^{29}Si MAS NMR spectrum of the parent zeolite modified with lanthanum, and this might be due to the lower lanthanum loading (shown in Fig. 1b). Based on Loewenstein's rule [24], the Si/Al ratio in the framework of the lattice shown in Table 2 can be obtained from the ^{29}Si MAS NMR spectra by using the equation

$$\frac{\mathrm{Si}}{\mathrm{Al}} = \frac{\sum_{n=0}^{4} I_n}{\sum_{n=0}^{4} (n/4) I_n},$$

where I_n is the intensity of the peak associated with $Q^4(n\mathrm{Al})$. It was calculated that the framework Si/Al ratio of both the parent HZSM-5 and the La/HZSM-5 was 21. This value is just a little bit higher than that from XRF analysis, owning to the existence of nonframework aluminum in the lattice, which is evidenced in the following ^{27}Al MAS NMR spectra. It indicates that the addition of lanthanum did not lead to dealumination of the lattice. On the other hand, the Si/Al ratio in the framework increased from 20 to 33 when the zeolite was modified by impregnation with orthophosphoric acid, in which about 37.5% of the total framework Al was removed from lattice (shown in Fig. 1c). It is obvious that the dealumination of zeolite proceeds under an acidic environment. The Si/Al ratio of the framework of the zeolite modified with both phosphorus and lanthanum, i.e., La-P/HZSM-5, was similar to that of the Si/Al ratio zeolite modified only by phosphorus (P/HZSM-5). After the parent zeolite HZSM-5 treated under 100% steam at 1073 K, it is clear that a new peak centered at −110.0 ppm appeared in the ^{29}Si MAS NMR spectra (Fig. 1a), which has been well recognized as the amorphous Si species [25]. The remaining signal became narrowed owing to a marked decrease in intensity of the signal at −107.4 ppm, which indicated dealumination of the zeolite [26]. Compared with

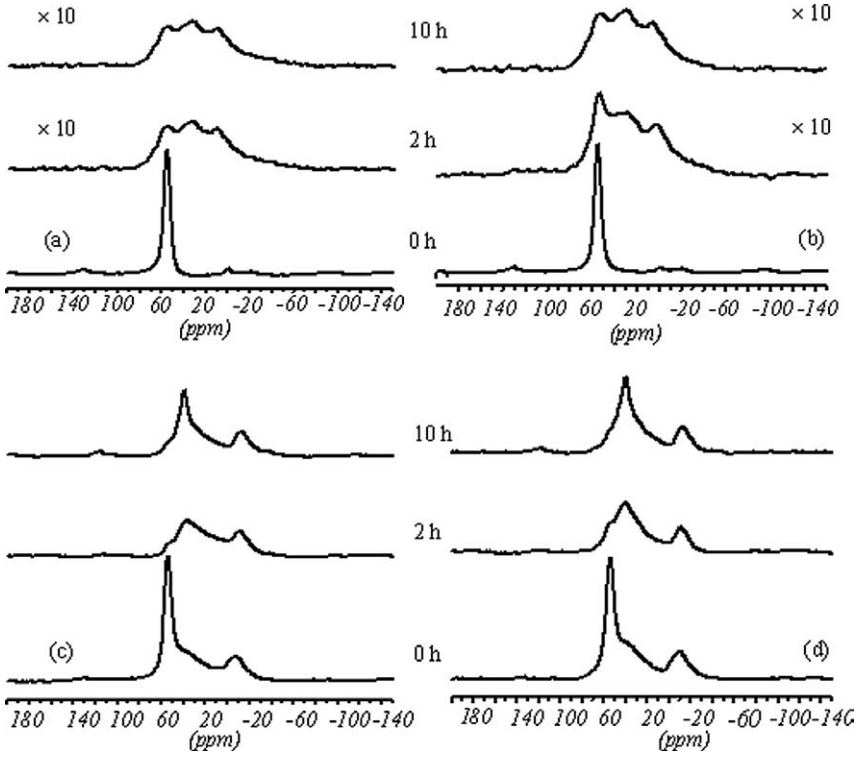

Fig. 3. ^{27}Al MAS NMR spectra of zeolites treated with 100% steam at 1073 K for different times: (a) HZSM-5, (b) La/HZSM-5, (c) P/HZSM-5, (d) La-P/HZSM-5.

the parent sample, more aluminum species were still maintained in the framework of the modified zeolites after hydrothermal treatment, as illustrated in the ^{29}Si MAS NMR spectra (see Fig. 1). The framework Si/Al ratios of the samples, especially for those impregnated with orthophosphoric acid, still maintained about 57 even after severe hydrothermal treatment for 10 h, which implied that the addition of phosphorus and lanthanum can efficiently retard the dealumination process under hydrothermal conditions. In their corresponding ^{1}H MAS NMR spectra (shown in Fig. 2), dealumination is also reflected after the samples treated at high temperature with steaming. Before hydrothermal treatment, four signals can be well distinguished in ^{1}H MAS NMR spectrum of HZSM-5 (Fig. 2a). The peaks at 1.6 and 4.0 ppm are normally assigned to the nonacidic hydroxyl groups and bridging hydroxyl groups, respectively. The resonance at 2.2 ppm is related to hydroxyl groups bonded to the extraframework aluminum. The broad peak at 6.0 ppm is ascribed to a second Brønsted acid site in HZSM-5 zeolite, which has an additional electrostatic interaction with the zeolite framework [27–29]. As a result of orthophosphoric acid impregnation, the intensity of the Brønsted acid decreased (Figs. 2c and d), which can be explained exclusively by a framework dealumination [30], which is in good agreement with the results of ^{29}Si MAS NMR spectra. It should be noted that POH from orthophosphoric acid can also contribute to the signal centered at 2.2 ppm in the ^{1}H MAS NMR spectra. Whereas the steaming treatment at 1073 K results in a fatal decrease in the intensity of all the signals, which indicated that dealumination occurred. On the other hand, the nonframework aluminum species condensed to the polymeric aluminum species, which caused the decrease of nonframework AlOH at 2.2 ppm [31]. Moreover, the vicinal hydroxyl groups (SiOH) can also dehydrate to form an intact Si–O–Si, which resulted in the decrease of silanols. Nevertheless, the remaining Brønsted acid sites still can be distinguished in the ^{1}H MAS NMR spectra of the samples modified by orthophosphoric acid (Figs. 2c and d), which implied the higher hydrothermal stability of the modified samples than parent zeolite.

3.3. ^{27}Al MAS NMR and ^{27}Al 3Q MAS NMR spectra of the samples

Fig. 3 shows the ^{27}Al MAS NMR spectra of the parent and modified samples before and after hydrothermal treatment. It exhibits an intense and sharp signal at 54.0 ppm in the ^{27}Al MAS NMR spectrum of the parent zeolite (see Fig. 3a), which is due to aluminum species in tetrahedral coordination (FAl^{IV}). An additional and weak peak centered at 0 ppm is also observed, which is normally assigned to octahedrally coordinated extraframework Al species ($NFAl^{VI}$) [32]. No changes were observed in the ^{27}Al MAS NMR spectrum of the La/HZSM-5 compared with that of parent zeolite (shown in Fig. 2b). It can be deduced that the framework of the sample modified with lanthanum was not changed, which is well in agreement with the results of ^{29}Si MAS NMR and XRD. The spec-

tra of the samples, P/HZSM-5 (Fig. 3c) and La-P/HZSM-5 (Fig. 3d) show a relatively narrow resonance at 54 ppm, but very broad resonances in 10–40 ppm range. Their assignment is confusing because of the overlapping. The peaks at 0–10 ppm are generally contributed to the octahedrally coordinated nonframework Al species and the $AlPO_4$ species. In order to remove the effect of second-order broadening from the central transition of half-integer quadrupolar nuclei to obtain pure absorption-mode lineshapes, the multiple-quantum magic-angle-spinning (MQMAS) NMR technique was used in our experiments. The ^{27}Al 3Q MAS NMR spectrum of P/HZSM-5 is presented in Fig. 4a. At least three Al species marked as A to C can be identified. Table 3 summaries the assignment of the peaks to the corresponding Al species. Signal A is attributed to tetrahedral Al sites corresponding to the peak at 54 ppm in 1D ^{27}Al MAS NMR spectra (shown in Fig. 4c), which is well known in the skeleton of the zeolite. The contour plot (signal B) corresponding to the isotropic chemical shift of 63.7 ppm is related to disordered tetrahedrally coordinated framework aluminum-oxygen species [3,33]. The larger SOQE of this signal indicates that the electronic environment about the Al is highly distorted owing to the very close interaction of P with framework Al. The signal C (δ_{iso} ^{27}Al = −17.2 ppm, SOQE = 3.94 MHz) is characteristic of the octahedrally coordinated nonframework Al nuclei in aluminum phosphates [32]. It is obvious that dealumination of the HZSM-5 zeolite occurred under acidic conditions, which led to the formation of nonframework aluminum phosphates. Compared with the sample P/HZSM-5, two new signals appeared, marked as D (δ_{iso} ^{27}Al = 52.0 ppm, SOQE = 7.75 MHz) and E (δ_{iso} ^{27}Al = −9.1 ppm, SOQE = 3.81 MHz), in the ^{27}Al 3Q MAS NMR spectrum of the La-P/HZSM-5 (shown in Fig. 4b). The peak position of signal D falls within the Al chemical shift region for tetrahedral framework Al. It is very likely that these Al species might experience a substantial electrical field gradient due to the nearest lanthanum and phosphorus. Signal E is also related to the octahedrally coordinated nonframework Al nuclei in aluminum phosphates. The signal of the remaining octahedrally coordinated Al in aluminum-oxygen species at 0 ppm was not identified, although it appeared in the ^{27}Al MAS NMR spectrum of the parent zeolite shown in Fig. 3a. This implies that the interaction of H_3PO_4 with extraframework aluminum of the zeolite might lead to the formation of different types of aluminum phosphate, which can be well distinguished in the ^{27}Al 3Q MAS NMR spectra, but they just exhibited as broad resonances in 1D ^{27}Al MAS NMR spectra.

After hydrothermal treatment at 1073 K for 2–10 h, the ^{27}Al MAS NMR spectra of all the samples indicate reduced intensities to various degrees for all signals, especially for those of the parent zeolite. These findings can be explained by the invisibility of the aluminum species in the NMR spectrum due to larger quadrupole couplings [22,34–37]. A new broad resonance centered around 30 ppm is also observed in the ^{27}Al MAS NMR spectra of the parent zeolite after hydrothermal treatment, which is assigned to penta-coordinated or disordered tetrahedral coordinated extraframework Al species. From the ^{27}Al MAS NMR spectra of the zeolite modified with La under the hydrothermal treatment condition (shown in Fig. 3b), we can deduce that the addition of lanthanum can partially resist the dealumination of the zeolite under severe conditions despite a lower lanthanum loading. From density-functional calculations, we found that the interaction between the Al and O atoms increased when the La^{3+} ion was introduced into the zeolite, thus enhancing the stability of the framework [38]. For the zeolite modified with orthophosphoric acid, the degree of dealumination was partially restrained after hydrothermal treatment. However, the FAl^{IV} species (related to 54 ppm) in the sample of La-P/HZSM-5 were better preserved at the first 2 h under steam conditions. After further stepwise steaming treatment, the peak intensity for the signal at 40 ppm increased, while that at 54 ppm decreased in both samples, P/HZSM-5 and La-P/HZSM-5 zeolites, and the intensity of octahedral Al was affected to a much lesser extent. Figs. 4c–f show the ^{27}Al 3Q MAS NMR spectra of the samples P/HZSM-5 and La-P/HZSM-5 under 100% steam at 1073 K. It is obvious that two identical signals F (δ_{iso} ^{27}Al = 56.6 ppm, SOQE = 8.16 MHz) and G (δ_{iso} ^{27}Al = 62.5 ppm, SOQE = 7.38 MHz) appeared. Very likely, the F and G signals are tetrahedrally coordinated Al species connected to the zeolite framework, with both P and Si as the nearest neighbors. It might be due to that one or two Si–O–Al bonds in the $(SiO)_4Al$ species were broken under severe conditions, and then the phosphorus occupied the silicon sites to coordinate with aluminum, leading to the formation of the $(SiO)_xAl(OP)_{4-x}$ species. With increasing time, another identical peak appeared (H), the isotropic chemical shift of which was centered at 39.5 ppm, and the value of SOQE was 1.23 (shown in Fig. 4e). More Si–O–Al bonds around Al had broken and the silicon sites were replaced by a phosphorus compound, until the framework Al was removed from lattice positions absolutely. From the ^{27}Al 3Q MAS NMR spectra of the samples treated for 10 h, we can observe a lowering tendency of this replacement when the parent zeolite was modified with both lanthanum and phosphorus. This means that the existence of lanthanum can restrict the replacement of silicon by phosphorus due to the enhancing of the interaction between the Al and O atoms.

Table 3
The parameters and assignment of different aluminum species

Signal	Coordination	δ_{iso}	SOQE (MHz)	Framework
A	4	60.4	3.26	Yes
B	4	63.7	6.83	Yes
C	6	−17.2	3.94	No
D	4	52.0	7.75	Yes
E	6	−9.1	3.81	No
F	4	56.6	8.16	Yes
G	4	62.5	7.38	Yes
H	4	39.5	1.23	No

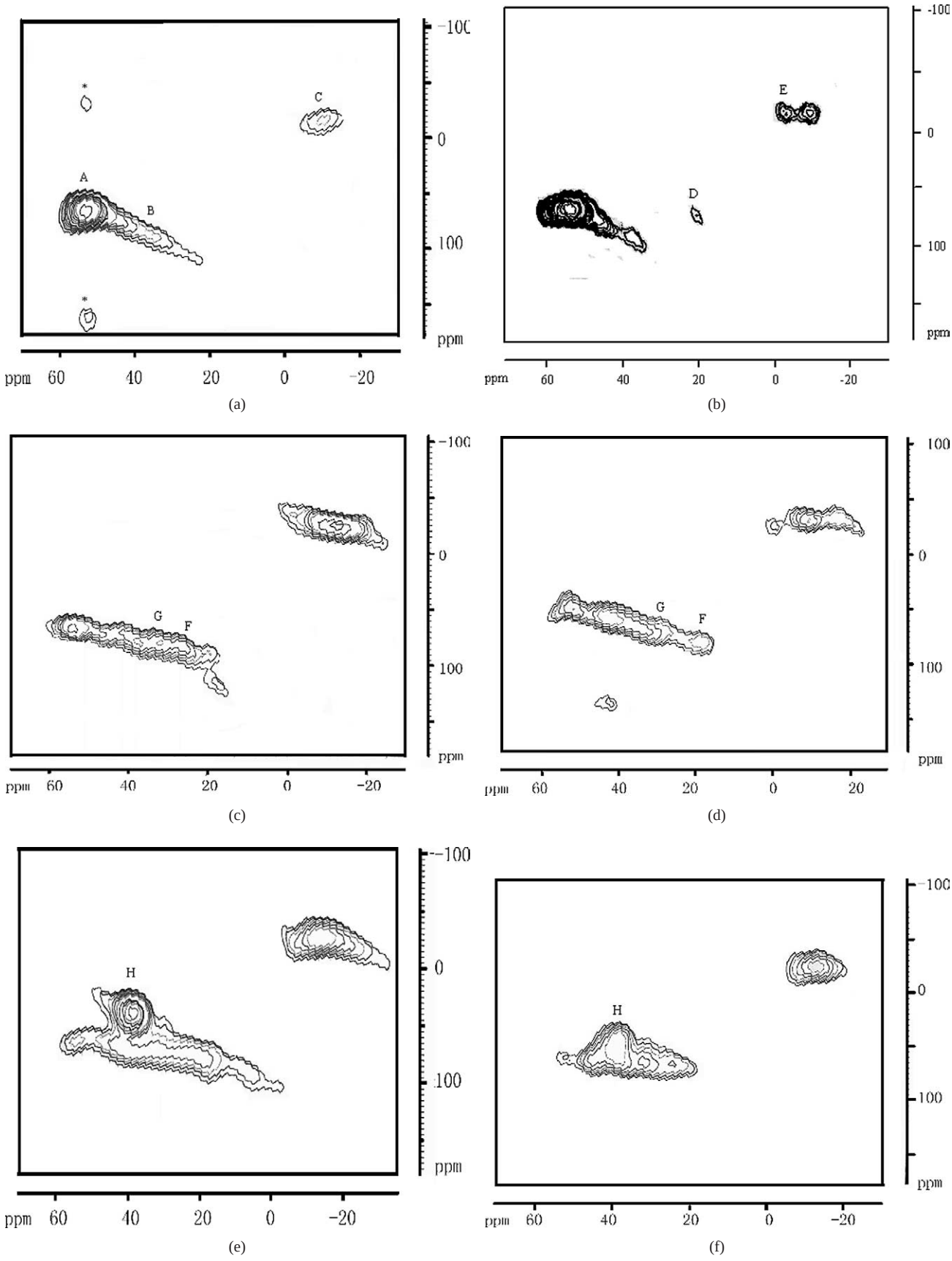

Fig. 4. Two-dimensional ^{27}Al 3Q MAS NMR spectra of (a) P/HZSM-5 (0 h), (b) La-P/HZSM-5 (0 h), (c) P/HZSM-5 (2 h), (d) La-P/HZSM-5 (2 h), (e) P/HZSM-5 (10 h), (f) La-P/HZSM-5 (10 h).

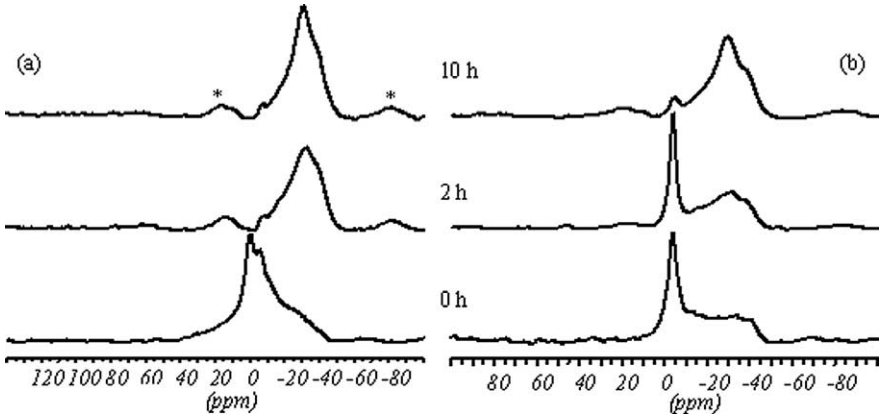

Fig. 5. ^{31}P MAS NMR spectra of zeolites treated with 100% steam at 1073 K for different times: (a) P/HZSM-5, (b) La-P/HZSM-5.

3.4. ^{31}P MAS NMR spectra of the samples

Fig. 5a illustrates the ^{31}P MAS NMR spectra of the P/HZSM-5 sample, which consisted of three identical peaks and a broad resonance. The peak at 0 ppm is associated with the excess phosphorus compound, which did not react with the framework aluminum [30,39]. The peak at −6 ppm is due to the phosphorus atoms in pyrophosphoric acid or due to the terminal $[PO_4]^{3-}$ groups in polyphosphoric species [30,33,40,41]. The resonance at −12 ppm represents the chemical shift usually obtained for middle groups in pyrophosphates or other short-chain polyphosphates [41]. The remaining broad resonance at −20 to −40 ppm normally contains signals of longer polymeric phosphate chains and extraframework aluminum phosphate as well as highly condensed polyphosphate species [42–44]. After the sample was hydrothermally treated at 1073 K for 2 h, the intensity of the low-field signals (0 ppm and −6 ppm) decreased, whereas that of the broad high field signal increased with a maximum at about −30 ppm, relating to extraframework aluminum phosphate. The broad resonance is attributed to $(SiO)_xAl(OP)_{4-x}$, which has been well distinguished by the ^{27}Al 3Q MAS NMR spectra. With increasing treatment time, the linewidth of the broad resonance was reduced, reflecting that more silicon sites were replaced by phosphorus, until the aluminum had escaped from the lattice completely to form extraframework aluminum phosphate. In comparison to the sample P/HZSM-5, there was no new resonance observed in the ^{31}P MAS NMR spectrum of the sample La-P/HZSM-5 (shown in Fig. 5b), except that no excess phosphorus compounds corresponding to 0 ppm were observed. After hydrothermal treatment for 2 h, there was just a little change observed in the ^{31}P MAS NMR spectrum of the sample La-P/HZSM-5. When the sample was treated for 10 h, the preserving of the linewidth in the broad resonance shown in Fig. 5b implies that there still existed different Al–O–P species. It indicates that the addition of lanthanum can effectively resist the Si–O–Al bond to be broken as well as the replacement of the silicon sites bounded to framework Al by phosphorus, and this is in good agreement with our results from the ^{27}Al 3Q MAS NMR spectra. In other words, there might be concerted interaction between lanthanum and phosphorus in the zeolite to limit dealumination from the lattice.

4. Conclusions

By employing XRD and solid-state MAS NMR techniques, we have investigated the hydrothermal stabilities of zeolite catalysts for residual oil selective catalytic cracking. It indicated that lanthanum can partially resist the dealumination of the HZSM-5 zeolite under 100% steam at 1073 K even at lower loading. 1D ^{27}Al and 3Q MAS NMR spectra showed that partial framework dealumination took place when the parent zeolite was impregnated by orthophosphoric acid, while the hydrothermal stability was enhanced even under severe conditions for a long time. It displayed that orthophosphoric acid interacted with the framework Al to form different Al species. Part of the Si–O–Al bonds in the tetrahedral coordinated framework Al species were broken instead such that phosphorus occupied the silicon sites to form the $(SiO)_xAl(OP)_{4-x}$ species. With increasing time under hydrothermal conditions, more silicon sites were substituted by phosphorous, till all the Al–O–Si bonds were broken to form extraframework Al species. Lanthanum played an important role in protecting more silicon sites around Al to be further replaced by phosphorous, which was also proved by the ^{31}P MAS NMR spectra. It has been shown that there exists concerted interaction between lanthanum and phosphorous atoms to resist dealumination from the lattice.

Acknowledgments

We are grateful for the support of The Foundation of Chinese Academy of Sciences (No. KGCX2-208-3) and The Ministry of Science and Technology of China (2003CB615806). The authors thank Mr. J. Jiao, Mr. H. Zheng, and Mr. X. Lan for helpful discussions.

References

[1] F.S. Xiao, G.S. Pang, T.H. Ji, X.P. Meng, W.Q. Pang, R.R. Xu, Appl. Catal. 133 (1995) 305.
[2] Z.M. Liu, P. Xie, J.L. Zhang, M.Z. Li, S.K. Zhu, G.W. Wang, Z.X. Zhang, J. Hu, J.G. Yang, CN patent 02157895.8.
[3] J. Sterte, J.E. Otterstedt, Appl. Catal. 38 (1988) 131.
[4] J.E. Otterstedt, Y.M. Zhu, J. Sterte, Appl. Catal. 70 (1991) 43.
[5] P. Gelin, T.D. Courieres, Appl. Catal. A 72 (1991) 179.
[6] B. Corma, W. Wojciechowski, Catal. Rev.-Sci. Eng. 27 (1985) 29.
[7] C.S. Tiantafillidis, N.P. Evmiridis, L.I. Nalbandian, A. Vasalos, Ind. Eng. Chem. Res. 38 (3) (1999) 916.
[8] W.W. Kaeding, C. Chu, L.B. Young, S.A. Butter, J. Catal. 69 (1981) 392.
[9] L.B. Young, S.A. Butter, W.W. Kaeding, J. Catal. 76 (1982) 418.
[10] J.A. Lercher, G. Rumplmayr, Appl. Catal. 25 (1986) 215.
[11] M.L. Costenoble, W.J. Mortier, J.B. Uytterhoeven, J. Chem. Soc., Faraday Trans. I 73 (1977) 466.
[12] C.D. Chang, C. Chu, R.F. Socha, J. Catal. 86 (1984) 289.
[13] G. Engelhardt, D. Michel, High-Resolution Solid-State NMR of Silicates and Zeolites, Wiley, New York, 1987.
[14] A.T. Bell, A. Pines, NMR Techniques in Catalysis, Dekker, New York, 1994.
[15] J.A. Van Bokhoven, A.L. Roest, D.C. Koningsberger, J.T. Miller, A.P. Nachtegaal, M. Kentgens, J. Phys. Chem. B 104 (2000) 6743.
[16] C.A. Fyfe, J.L. Bretherton, L.Y. Lam, Chem. Commun. (2000) 1575.
[17] D. Ma, X. Han, S. Xie, X. Bao, H. Hu, S.C.F. Au-Yeung, Chem-A. Eur. J 8 (1) (2002) 162.
[18] L. Frydman, J.S. Harwood, J. Am. Chem. Soc. 117 (1995) 5367.
[19] A. Medek, J.S. Harwood, L. Frydman, J. Am. Chem. Soc. 117 (1995) 12779.
[20] M. Sugimoto, H. Kasuno, K. Takatsu, N. Kawata, Zeolite 7 (1987) 503.
[21] J.C.C. Chan, Concepts Magn. Reson. 11 (1999) 363.
[22] E. Brunner, H. Ernst, D. Freude, J. Catal. 127 (1991) 34.
[23] J.A. Van Bokhoven, A.L. Roest, D.C. Koningsberger, J. Phys. Chem. B 104 (2000) 6743.
[24] W. Loewensten, Am. Miner. 39 (1954) 92.
[25] K.F.M.G.J. Scholle, W.S. Veeman, P. Frenken, G.P.M. van der Velden, Appl. Catal. 17 (1985) 233.
[26] S.M. Campbell, D.M. Bibby, J.M. Codington, R.F. Howe, R.H. Meinhold, J. Catal. 161 (1996) 338.
[27] M. Hunger, Catal. Rev.-Sci. Eng. 39 (1997) 6345.
[28] L.W. Beck, J.L. White, J.F. Haw, J. Am. Chem. Soc. 116 (1994) 9657.
[29] E. Brunner, J. Mol. Struct. 335 (1995) 61.
[30] J. Caro, M. Bulow, M. Derewinski, J. Haber, M. Hunger, J. Karger, H. Pfeifer, W. Storek, B. Zibrowius, J. Catal. 124 (1990) 367.
[31] R.D. Shannon, K.H. Gardner, R.H. Stadey, G. Bergeret, P. Gallezot, A. Auroux, J. Phys. Chem. 89 (1985) 4778.
[32] J. Sanz, V. Fornes, A. Corma, J. Chem. Soc., Faraday. Trans. 84 (1988) 3113.
[33] G. Lischke, R. Eckelt, H.G. Jerschkewitz, B. Parllitz, E. Schreier, W. Storek, B. Zibrowius, G. Ohlmann, J. Catal. 132 (1991) 229.
[34] J. Sanz, J.M. Campelo, J.M. Marinas, J. Catal. 130 (1991) 642.
[35] K.J.D. Mackenzie, I.W.M. Brown, R.H. Meinhold, M.E. Bowden, J. Am. Chem. Soc. 68 (1983) 293.
[36] S.M. Campbell, D.M. Bibby, J.M. Coddington, R.F. Howe, R.H. Meinhold, J. Catal. 161 (1996) 338.
[37] C.A. Fyfe, J.L. Bretherton, L.Y. Lam, J. Am. Chem. Soc. 123 (22) (2001) 5285.
[38] G. Yang, Y. Wang, D.H. Zhou, J.Q. Zhuang, X.C. Liu, X.W. Han, X.H. Bao, J. Chem. Phys. 119 (18) (2003) 9765.
[39] G. Seo, R. Ryoo, J. Catal. 124 (1990) 224.
[40] A.R. Grimmer, U. Haubenreisser, Chem. Phys. Lett. 99 (1983) 487.
[41] T.M. Duncan, D.C. Douglass, Chem. Phys. 87 (1984) 339.
[42] D. Muller, E. Jahn, G. Ladwig, Chem. Phys. Lett. 109 (1984) 332.
[43] C.S. Blackwell, R.L. Patton, J. Phys. Chem. 88 (1984) 6135.
[44] E.C. Drcanio, J.C. Edwards, T.R. Scalzo, D.A. Storm, J.W. Bruno, J. Catal. 132 (1991) 498.